

# Multi-Platform Observations and Numerical Simulations to Understand Meso and Submesoscale Processes: A Case Study of Vertical Velocities in the Western Mediterranean

Simón Ruiz<sup>1</sup>, Amala Mahadevan<sup>2</sup>, Ananda Pascual<sup>1</sup>, Mariona Claret<sup>3</sup>, Joaquín Tintoré<sup>1,4</sup>,  
and Evan Mason<sup>1</sup>

<sup>1</sup>*Instituto Mediterráneo de Estudios Avanzados (CSIC-UIB), Esporles, Spain;* <sup>2</sup>*Wood Hole Oceanographic Institution, Woods Hole, MA, USA;* <sup>3</sup>*Joint Institute for the Study of the Atmosphere and Ocean, University of Washington, Seattle, WA, USA;* <sup>4</sup>*Balearic Islands Observing and Forecasting System (SOCIB), Palma de Mallorca, Spain*

*In this chapter we provide a description of an intense ocean front and an anomalous anticyclonic eddy in the Western Mediterranean. We use observations from two multi-platform experiments carried out in the eastern Alboran Sea and in the northern Balearic Islands. We diagnose mesoscale vertical motion ( $\pm 1\text{-}10 \text{ m/day}$ ) associated with these ocean structures using quasi-geostrophic dynamics. A unique characteristic of both field experiments is the combination of conventional in situ measurements from ships with high-resolution observations using autonomous underwater vehicles (gliders). For the eastern Alboran Sea, we also use a high-resolution numerical model that is initialized with hydrographic data (0.5–1 km resolution) from gliders. Numerical simulations show that lateral buoyancy gradients are large enough to trigger submesoscale mixed layer instabilities. Results from the model illustrate that a mixed layer tracer subducts to form vertical intrusions extending to depths of 80–90 m, which is in agreement with remarkable subduction events of chlorophyll and oxygen captured by ocean gliders.*

---

## Introduction

Mesoscale (10–100 km) and submesoscale (1–10 km) ocean structures play a major role in the redistribution of properties such as heat, salt, and biochemical tracers, with a significant impact on the ocean's primary productivity (Levy et al., 2001; Ramachandran et al., 2004; Omand et al., 2015). The dynamics associated with these features result in enhanced vertical velocities and mixing, as well as stratification, on time scales that range from a few days to several months and from a few kilometers to 100 km (Klein and Lapeyre, 2009; Ruiz et al., 2009a; Pascual et al., 2015; McWilliams, 2016). In the last 20 years, satellite altimetry has

---

Ruiz, S., et al., 2018: Multi-platform observations and numerical simulations to understand meso and submesoscale processes: A case study of vertical velocities in the Western Mediterranean. In "New Frontiers in Operational Oceanography", E. Chassignet, A. Pascual, J. Tintoré, and J. Verron, Eds., GODAE OceanView, 117–130, doi:10.17125/gov2018.ch05.

helped improve our understanding of surface ocean circulation (e.g., Le Traon, 2013), leading to major breakthroughs such as the quantification of eddy kinetic energy (Pascual et al., 2006) and eddy identification and tracking (Chelton et al., 2011; Mason et al., 2014) at scales  $>100$  km. However, the present constellation of altimeters still lacks enough resolution to cover scales shorter than 100 km, typical of ubiquitous mesoscale and submesoscale features such as fronts, meanders, eddies, and filaments. Increasing our knowledge about the relationship between the physical, chemical, and biological processes in the upper ocean is essential for understanding and predicting the ocean and the functioning of marine ecosystems. High-resolution observations (both in situ and satellite) and multi-sensor approaches (e.g., Shcherbina et al., 2015) are necessary to advance our knowledge and prediction of the ocean.

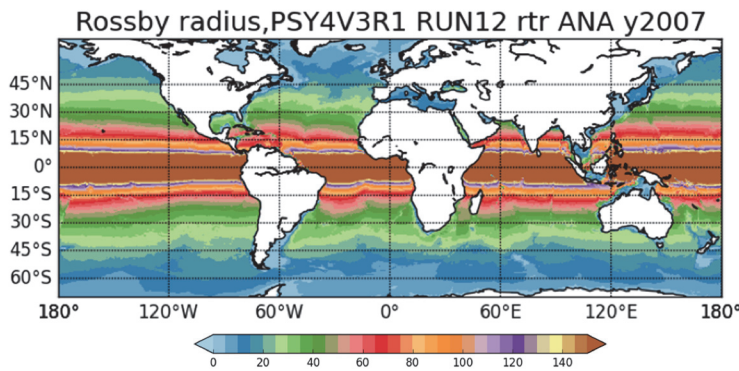


**Figure 5.1.** Rossby radius of deformation (km) from global operational model (Courtesy of Angélique Melet, Mercator-Ocean).

The Mediterranean Sea is considered an accessible and reduced-scale ocean laboratory where most of the processes that are present in different regions of the global ocean can be investigated at a smaller scale, including deep convection (Herrmann et al., 2009), shelf-slope exchanges (Bethoux and Gentili 1999), thermohaline circulation and water mass interaction (Schröder et al., 2006), and mesoscale and sub-mesoscale dynamics (Bosse et al., 2017). In the context of ocean variability in the Mediterranean Sea, we see that the Rossby radius of deformation is smaller in this semi-closed sea than in other areas of the global ocean located at a similar latitude (Fig. 5.1).

Mesoscale and submesoscale features such as eddies and filaments (Fig. 5.2) interact with each other on the sub-basin and basin scales (Allen et al., 2001; Ruiz et al., 2009a). This amalgam of intricate processes requires high-resolution and comprehensive observations to be fully understood (Pascual et al., 2017).

---

## Meso and Submesoscale Processes: Multi-platform Observations and Numerical Simulations

---

### Methods and data

The vertical velocity ( $w$ ) in the ocean is generally four orders of magnitude smaller than horizontal velocity and, therefore, it is difficult to obtain direct measurements of vertical velocity (Klein and

Lapeyre, 2009). Vertical velocity can be diagnosed resolving the continuity equation in primitive equation numerical models; however, this approach cannot be followed using observations since instrumental error is as large as the magnitude of the variable ( $w$ ) to estimate. In the 1990s and the beginning of the 21<sup>st</sup> century, a common approach to diagnose the vertical motion associated with mesoscale eddies was the use of simplified diagnostic models from two-dimensional (2D) and/or three-dimensional (3D) gridded density and geostrophic fields (Tintoré et al., 1991; Pollard and Regier, 1992; Pinot et al., 1996). The use of the quasi-geostrophic (QG) approximation has led to a better understanding dynamics of physical mesoscale processes in the upper ocean (Rudnick, 1996; Buongiorno-Nardelli et al., 2012; Ruiz et al., 2014) and the coupling between physical and biogeochemical processes (Rodríguez et al., 2001; Allen et al., 2005).

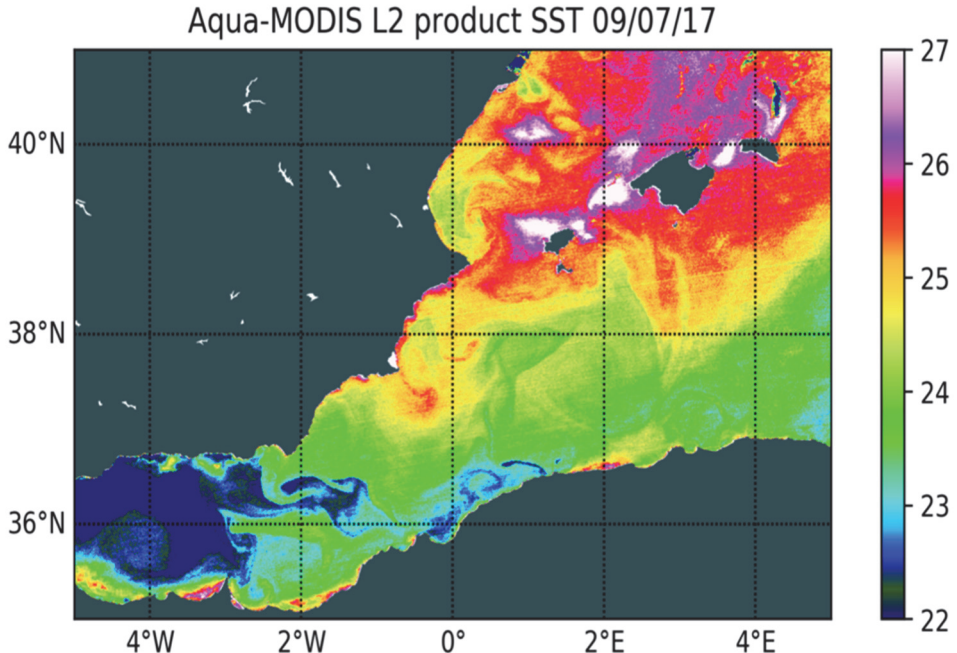


**Figure 5.2.** Sea surface temperature (SST) image (°C) corresponding to 09 July 2017 covering the western Mediterranean Sea. Fine-scale features are observed due to the interactions of the entrance of fresh and cold Atlantic water (blue) and the more saline and warmer resident Mediterranean water (green).

The diagnostic QG omega equation is directly obtained from the QG vorticity and thermodynamic equation (Hoskins et al., 1978):

$$f^2 \frac{\partial^2 w}{\partial z^2} + \left( \frac{\partial^2}{\partial x^2} + \frac{\partial^2}{\partial y^2} \right) (N^2 w) = \nabla_h \cdot \mathbf{Q} \quad (1)$$

where

$$\mathbf{Q} = \left[ 2f \left( \frac{\partial V}{\partial x} \frac{\partial U}{\partial z} + \frac{\partial V}{\partial y} \frac{\partial U}{\partial z} \right), -2f \left( \frac{\partial U}{\partial x} \frac{\partial U}{\partial z} + \frac{\partial U}{\partial y} \frac{\partial V}{\partial z} \right) \right]$$

and  $(U, V)$  are the geostrophic velocity components,  $f$  is the Coriolis parameter, and  $N$  is the buoyancy frequency. The vertical velocity ( $w$ ) can be estimated considering a set of boundary conditions for  $w$  and using a 3D snapshot of the density field. In the examples shown in this chapter,

$w=0$  at the upper and lower boundaries and Neumann conditions at the lateral boundaries. The 3D density field (2 x 2 km horizontal resolution and every 5 m in the vertical) is obtained applying an optimal statistical interpolation (OSI) to hydrographic data.

### The AlborEx experiment: An intense front

A major intensive, multi-platform and multidisciplinary experiment was completed in May 2014 as a part of PERSEUS (Policy-oriented marine Environmental Research for the Southern European Seas) EU-funded project, led by the Consejo Superior de Investigaciones Científicas (CSIC) and with strong involvement of the Balearic Islands Coastal Observing and Forecasting System (SOCIB), the Instituto Nazionale di Oceanografia e di Geofisica Sperimentale (OGS), the Consiglio Nazionale delle Ricerche (CNR), Woods Hole Oceanographic Institution (WHOI), and McGill University. The multi-platform AlborEx experiment (Fig. 5.3) conducted over eight days, included 25 drifters, two gliders, three Argo floats, one ship, and 50 scientists. The week-long experiment was designed to capture the intense but transient vertical motion associated with mesoscale and submesoscale features in order to fill gaps in our knowledge connecting physical processes to ecosystem response (Ruiz et al., 2015).

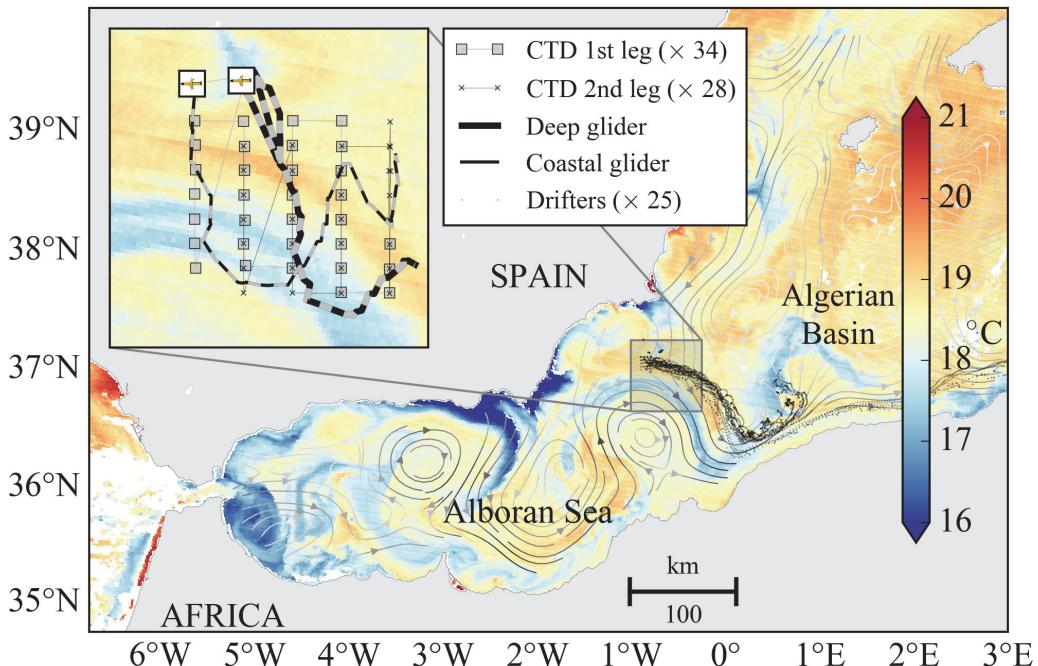


**Figure 5.3.** SST (MODIS-Aqua) for 29 May 2014 with conductivity, temperature, and depth (CTD) casts, glider and drifter paths during AlborEx experiment. The gray lines correspond to streamlines computed from absolute dynamic topography from gridded altimeter fields (Copernicus Marine Environment Monitoring Service or CMEMS-SLTAC). (From Pascual et al., 2017).

In the Western Mediterranean, the transition region between the Alboran Sea and the Algerian sub-basin to the east is characterized by strong fronts and mesoscale anticyclonic eddies. Transient fronts, such as the Almería-Orán front, separate Atlantic water flowing into the Mediterranean Sea

and resident Mediterranean Water that intrudes southwestward along the Spanish coast. Ruiz et al. (2009a) reported mesoscale (~100 km) quasi-geostrophic vertical velocities of the order  $\pm 1$  m/day estimated from a combination of altimetry and glider observations south of Cartagena, although higher velocities (up to  $\pm 20$ -25 m/day) can be assumed for smaller meso- and submesoscale structures embedded within the front (Allen et al., 2001).

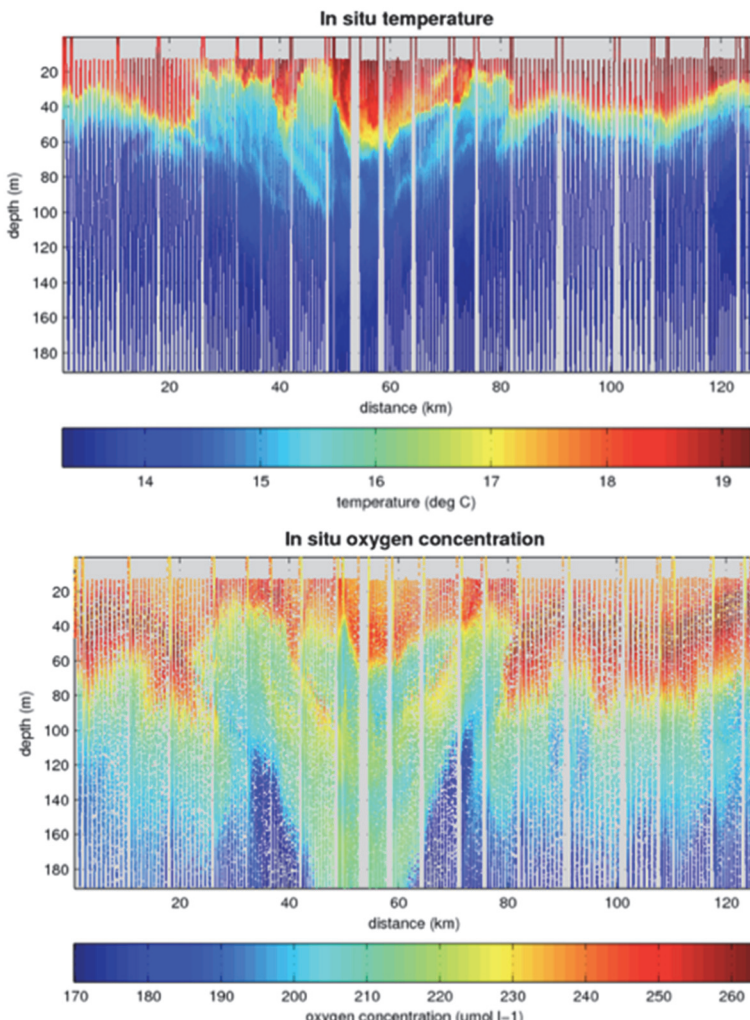


**Figure 5.4.** Vertical section of temperature and oxygen from the coastal glider.

#### Autonomous underwater vehicles

Two ocean gliders were able to sample at high-resolution the frontal zone. The coastal glider reached a maximum depth of 200 m and was configured to collect hydrographic and biochemical data at about 0.5 km, while resolution of data from the deep glider was at a depth of ~1 km along-track (data not shown) and it collected data from the surface to 500 m. Fig. 5.4 shows the temperature and oxygen data from the coastal glider. Subduction of small filaments (less than 10

km wide) was observed in different parts of the sampled area suggesting exchanges of properties from the upper layer to the ocean interior

### Ship CTDs and a Vessel-Mounted Acoustic Doppler Current Profiler (VM-ADCP)

Conductivity, temperature, and depth (CTD) data along with data from an Acoustic Doppler Current Profiler (ADCP) were gathered from the R/V SOCIB. All physical in situ data were quality-controlled (see Ruiz et al., 2015, for further details). The exact location of the CTD stations was fixed based on the presence of mesoscale and submesoscale features in SST data from remote sensing. The maximum depth reached during all of the CTD casts was 600 m and water samples were collected at each station at the following depths: 5, 20, 40, 60, 90, 100, 120, 150 m. Salinity samples were collected at different depths in one of two stations. An additional sample at 350 m was collected at certain stations for salinity calibration. The first CTD survey consisted of 34 CTD casts distributed over five north/south legs, performed 26-27 May 2014 (Fig. 5.3). During the second survey, 28 CTD casts were conducted on 29-30 May 2014 in almost the same positions as those performed during the first survey (Fig. 5.3).

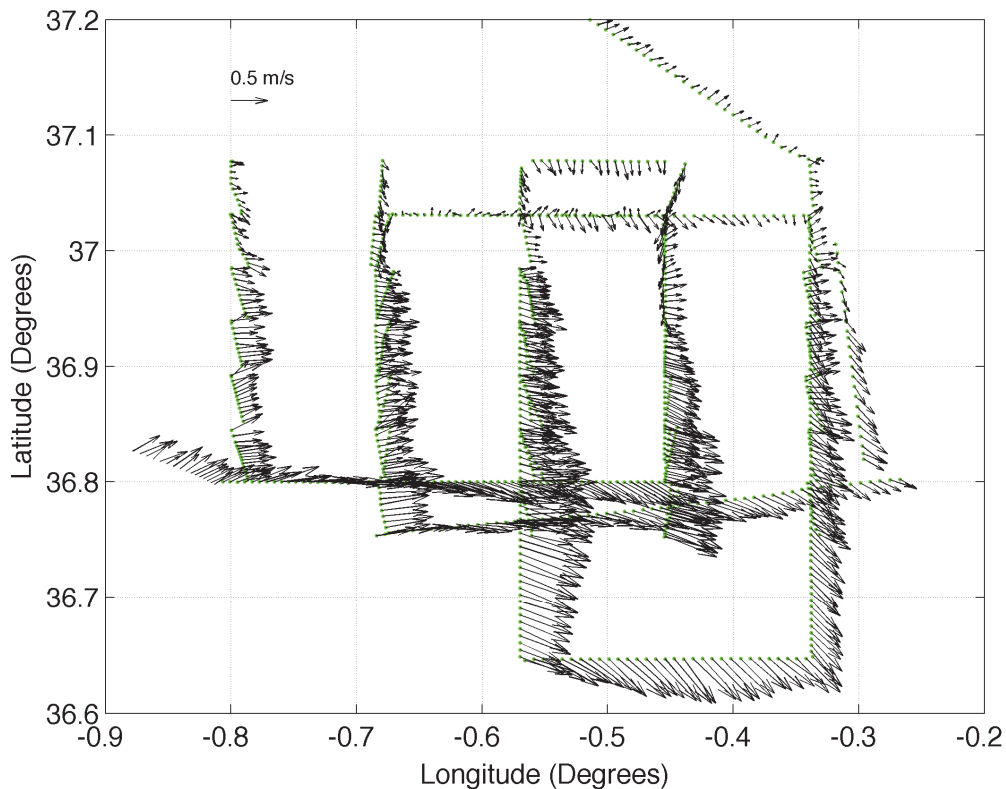


**Figure 5.5.** Velocity field (cm/s) from VM-ADCP at 48 m depth.

Direct current measurements were obtained from a VM-ADCP 153kHz, with an accuracy of about 1 cm/s. Original profiles were collected every two minutes resulting in approximately one profile every 0.5 km. In the vertical, data were also averaged over 8 m depth bins. Velocity from the first bin (16 m depth) reached values near 1 m/s (Fig. 5.5). It is worth noting that mean

geostrophic flow at 50 m depth (Fig. 5.6) was smaller ( $\sim 40$  cm/s) than the velocity from the VM-ADCP, which is about 50 cm/s (not shown). That is to be expected since the VM-ADCP measured actual velocity, including all velocity components.

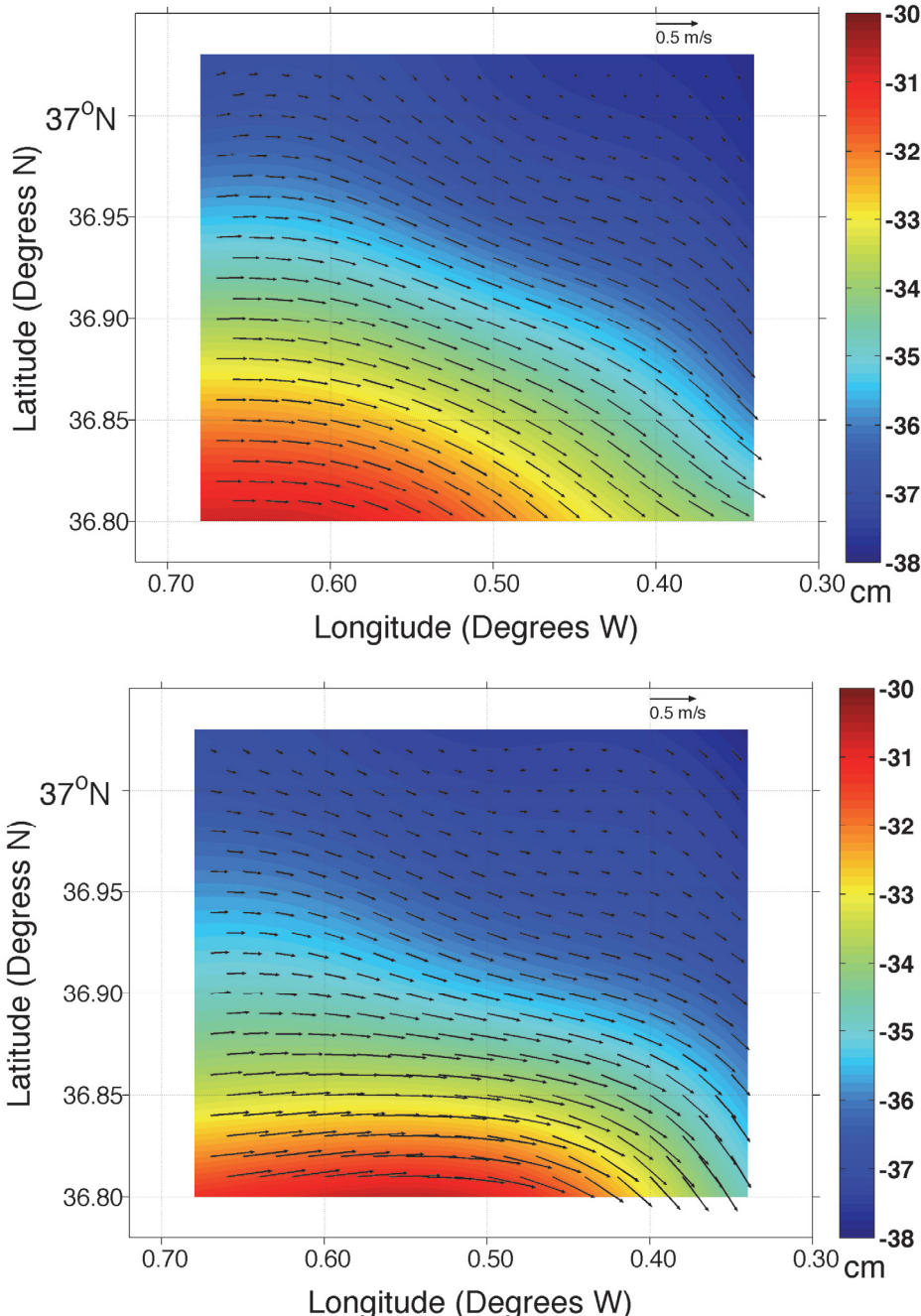


**Figure 5.6.** Dynamic height (cm, background colour) and geostrophic velocity (cm/s, vectors) at 50 m depth from ship-CTD survey 1 (left) and ship-CTD survey 2 (right). A reference level of no motion is assumed at 600 m depth (From Pascual et al., 2017).

Using the ship CTD data, a 3D density field was diagnosed and used to estimate the vertical velocity following the quasi-geostrophic approach described above (Eq. 1). On average, the magnitude of  $qg\omega$  from observations is about  $\pm 10$  m/day. The pattern is coherent having upwelling/downwelling upstream/downstream of the flow, however these vertical velocities are associated to structures larger than 20 km (Ruiz et al., pers. comm.). Potential contributions from smaller structures that were revealed by gliders (Fig. 5.4) have been filtered out in the QG analysis using a low-pass filter (Pedder, 1993).

### Numerical modelling

To explore the role of fine-scale features (< 20 km) in enhancing vertical transport at the front, a Process Ocean Study Model (PSOM, <https://github.com/PSOM>, Mahadevan et al., 1996) was used. Atmospheric forcing is not included in the model configuration in order to isolate and evaluate the particular role of the lateral density gradients. Flow remains statically, inertially, and symmetrically stable during the time period of the analyses. Domain is a periodic channel along the zonal direction (120 km) meridional dimension (200 km), lateral resolution (500 m). The vertical extent is 550 m ( $\sim 3$  m vertical resolution). A front defined by an encounter with Mediterranean and Atlantic waters is initialized in thermal-wind balance using a hydrographic glider section extended with 2 km-resolution output from the Western Mediterranean Operational forecasting system (Juza et al., 2016). A passive tracer was implemented homogeneous within the mixed layer, the depth of which is defined by a density criterion (a difference of  $0.01 \text{ kg m}^{-3}$  from the surface) in order to investigate vertical intrusions and subduction events below it.

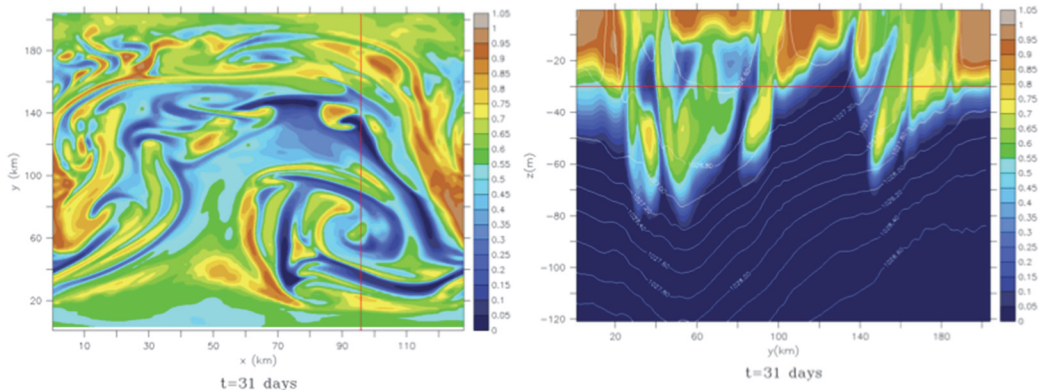


**Figure 5.7.** Horizontal section at 30m depth (top) and vertical section (bottom) of tracer after 31 days of simulation from PSOM model (resolution 500 m). Contours correspond to isopycnals.

Numerical simulations show the presence of mesoscale feature and fine-scale filaments. Mixed layer tracer subducts form vertical intrusions extending to depths of 80-90 m that become narrow filaments in the horizontal flow (Fig. 5.7). The intrusion of surface water occurs predominantly in regions of weak stratification (Ruiz et al., 2016, pers. comm.). Upwelling of tracer-free water occurs alongside downwelling and is less intense but highlights the subducted tracer.

## SINOCOP Experiment: A moderate anticyclonic eddy

The SINOCOP (Towards an integrated System of Coastal Operational Oceanography) experiment took place 12–18 May, 2009 covering a study area of 50 x 40 km<sup>2</sup>. The multi-platform experiment consisted of two Slocum gliders operated simultaneously and in combination with drifters, CTDs from ships, and remote sensing north of Mallorca Island (Fig. 5.8).

The scientific motivation of this experiment was to develop new methodologies to diagnose the 3D dynamics of the ocean using a multi-sensor approach in combination with numerical models. Particular attention was paid to the formation, evolution, and decay of mesoscale variability (and fine-scale features) associated with instabilities of the Balearic current, the main oceanographic feature that is found along the northwest coast of Mallorca Island (Western Mediterranean).

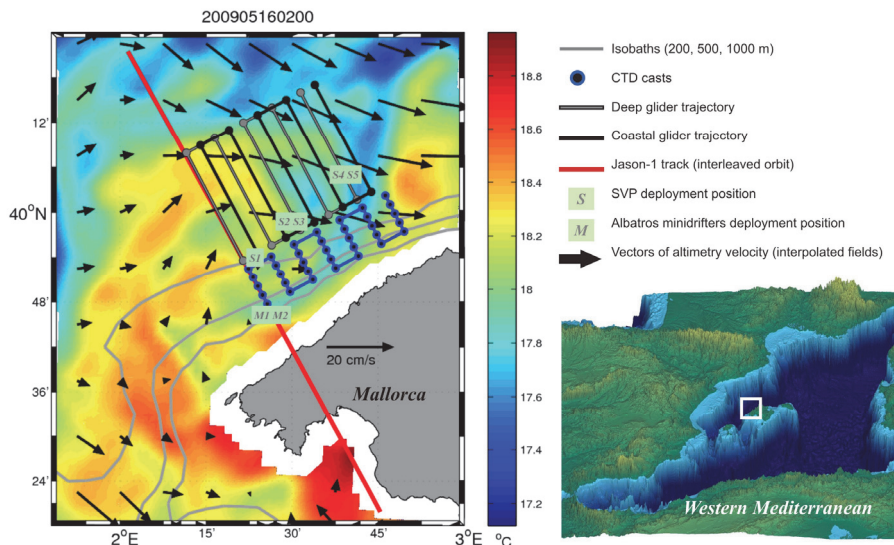


**Figure 5.8.** Study area during the multi-platform SINOCOP experiment.

### Gliders and ship CTDs

Two Slocum gliders, one shallow and one deep, were used. The shallow glider was configured to operate between the surface and 200 m, while the deep glider was set up to reach 600 m in order to meet the scientific objective of the experiment. The net horizontal speed of these vehicles is about 1 km/h, taking into account data transmission when they are at surface. During one week, 811 hydrographic (temperature and salinity) and biogeochemical measurements (turbidity, oxygen and chlorophyll) were registered. Gliders were set up to gather data when descending and ascending, resulting in a final horizontal resolution along-track of 0.5 km for the coastal glider, around 1.1 km for the deep glider, and at about 4 km between adjacent tracks. Final profiles were averaged in the vertical every 1 m. Regarding the glider data processing, special attention was paid to the thermal lag correction, which was applied following a specific procedure developed for gliders (Garau et al., 2010).

Twenty-four CTD casts (SeaBird-19 probe) were performed from IMEDEA coastal ship. The sampling covered the coastal zone between the isobaths of 200 m and 1000 m. The distance between stations was 2.5 km along the same transect and 6.5 km between consecutive transects. Standard CTD processing was applied and final profiles were 1 m averaged in the vertical (see Pascual et al., 2009 for further details).

## Drifters

In order to measure the surface currents, five Surface Velocity Program (SVP) ClearWater drifters were deployed in the study area. Each drifter was composed of a surface buoy with a subsurface drogue attached and centered at 15 m depth (Lumpkin and Garzoli, 2005), which guaranteed the flow of the drifter with the ocean currents (minimizing the wind effect). Positioning time series from drifters were linearly interpolated every six hours and a low-pass filter with a 36-hour cut-off frequency was applied in order to remove inertial oscillations. A velocity following the path of the drifters was computed by time differencing the processed 6-hourly positions. Finally, the time series were sub-sampled every 24 hours to obtain a daily product.

## Remote sensing: altimetry and SST

Two-dimensional interpolated gridded fields, currently delivered by the AVISO web server, were used in this experiment. The gridded fields are specific to the Mediterranean Sea and are computed on a regular  $1/8^\circ$  grid using a suboptimal space/time optimal interpolated analysis. Regarding SST satellite data, raw images at 1.2 km resolution acquired and processed by GOS-ISAC(CNR) as well as 6-hour averaged images at 2 km spatial resolution from EUMETSAT web server were available during the experiment.

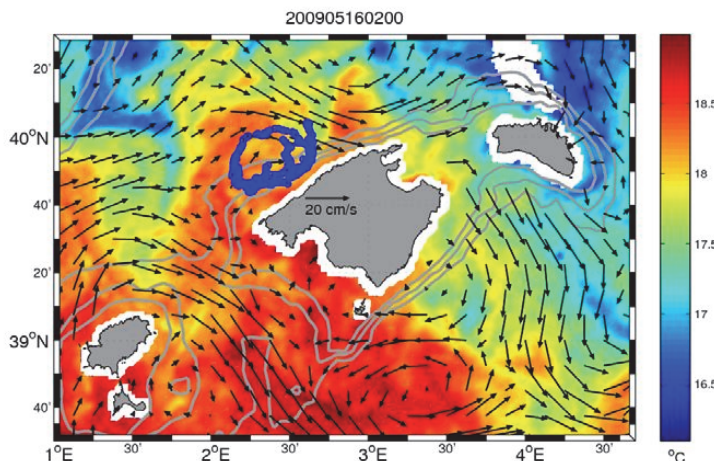


**Figure 5.9.** Drifter trajectories (blue). Arrows correspond to absolute geostrophic currents from altimetry and the color bar is SST. Isobaths (gray lines) are 200 m, 500 m, and 1000 m.

Relative fresh water from Atlantic origin (37.4) was not detected near the coast, as was found in the previous studies (Ruiz et al., 2009b). Instead, Mediterranean water (with salinity of about 38.4) was dominant in the study area. Analysis of in situ and remotely sensed observations revealed the presence of an anomalous anticyclonic eddy  $\sim 40$  km in diameter near the northwest coast of Mallorca Island (Fig. 5.9). This structure blocked the usual path of the Balearic Current along the

coast, deflecting the main northeastward flow to the north. From drifter data analysis, horizontal velocities associated with the eddy were estimated to be about 20 cm/s. Comparisons of drifter and altimetry data revealed that altimeter geostrophic currents derived from gridded products do not have sufficient resolution for the detection of these kinds of small mesoscale and submesoscale features (Fig. 5.9).

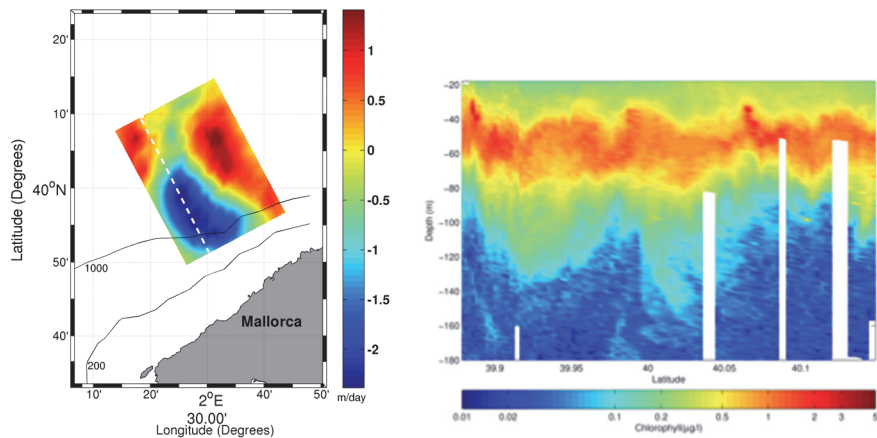


**Figure 5.10.** Left: QG vertical velocity (m/day) at 100 m depth estimated from hydrographic data (ship-CTD and glider-CTD). The white dashed line indicates the location of vertical chlorophyll ( $\mu\text{g/l}$ ) section (right) from the first transect of coastal glider.

Hydrographic data from the ship's CTD and derived geostrophic velocities were interpolated in a regular grid at 2 km resolution using an optimal interpolation scheme. Then, the Omega equation (Eq. 1) was solved setting  $w = 0$  at the upper and lower boundaries and Neumann conditions at the lateral boundaries. The anticyclonic eddy sampled had associated a vertical motion of about  $\pm 2$  m/day (Fig. 5.10). Preliminary analysis showed a sinking motion in the center of the eddy that may indicate an early stage of formation of the anticyclonic eddy. A more complete analysis of the whole dataset is in progress, including the modelling of this kind of mesoscale structure.

## Summary and Perspectives

The AlborEx and SINOCOP multi-platform and multidisciplinary experiments are examples of integrated multi-platform approaches to investigate the three-dimensional state of the ocean. Although there are still some limitations in terms of spatial coverage (e.g., ocean gliders)—the lack of repeated high-resolution in situ measurements or low resolution of altimetry—the examples provided in this chapter represent a step forward in the direction of combining multiple sensors to further improve our understanding of ocean dynamics (D'Asaro et al., 2011). We have shown that for diagnosis of the vertical motion, which is a key variable for the ecosystem functioning, both field and numerical studies are necessary. Vertical velocities associated with mesoscale eddies derived from observations are in the range of 1–10 m/day and can be responsible for the spatial distribution of biogeochemical parameters such as chlorophyll (Pascual et al., 2015; Olita et al.,

2017; Mason et al., 2017). Fine-scale features can enhance the vertical exchange up to 20–30 m/day as was demonstrated in Mahadevan et al. (2006). Finally, and no less important, the AlborEx and SINOCOP experiments are examples of collaborative joint efforts between scientists, students, and technicians that encourage knowledge exchanges at national and international level.

To better evaluate the vertical and horizontal exchanges and interactions at meso- and submesoscale, we need to improve the coverage and resolution of in situ and remote sensing observational data (e.g., the Surface Water and Ocean Topography or SWOT altimeter mission) while increasing the resolution of numerical models capable of resolving fine-scale processes. The SWOT mission is scheduled to be launched in 2020 and the objectives of the altimeter mission are to characterize the ocean mesoscale and submesoscale circulation determined from ocean surface topography at spatial resolutions of 15 km. This represents a resolution one order of magnitude higher than can be resolved with present-day altimeters (Fu and Ferrari, 2008; Gómez-Navarro et al., 2018). New in situ autonomous platforms are also contributing to the measurement of fine-scale velocities in the ocean (Shcherbina et al., 2018; Jaffe et al. 2016) and exploration of submesoscale dynamics.

## Acknowledgements

The AlborEx experiment was conducted in the framework of PERSEUS EU-funded project (Grant agreement no: 287600) with substantial support from SOCIB. Glider operations were partially funded by JERICO FP7 projects. We would like to thank all the crew on board R/V SOCIB for their efficient collaboration during the Alborex experiment and all scientist that have contributed to the discussion of results (Charles Troupin, Arthur Capet, Antonio Olita, Antonio Tóvar-Sánchez, Pierre-Marie Poulain, John Allen). SINOCOP project is an Intramural project funded by Spanish National Research Council. We would like to extend especial thanks to Bruno Buongiorno Nardelli, Miguel Martínez-Ledesma, Bartolomé Garau, Kristian Sebastian, Enrique Vidal, Jérôme Bouffard and Romain Escudier for their efficient work during the SINOCOP experiment. E. Mason contract was partially funded by the Copernicus Marine Environment Monitoring Service (CMEMS) MedSUB project. This study is also a contribution to the PRE-SWOT project (CTM2016-78607-P) funded by the Spanish Research Agency and the European Regional Development Fund (AEI/FEDER, UE).

## References

- Allen, J. T. et al. (2005), Diatom carbon export enhanced by silicate upwelling in the northeast atlantic. *Nat.* 728–732. doi:10.1038/nature03948.
- Allen, J. T., D. A. Smeed, J. Tintoré, and S. Ruiz (2001), Mesoscale subduction at the Almeria-Oran front. Part 1: Agesotrophic flow, *J. Mar. Syst.*, 30, 263– 285, doi:10.1016/S0924-7963(01)00062-8.
- Bethoux, J.P., Gentili, B. (1999), Functioning of the Mediterranean Sea: past and present changes related to freshwater input and climate changes. *J. Mar. Syst.* 20, 33–47.
- Bosse, A., Testor, P., Mayot, N., Prieur, L., D'Ortenzio, F., Mortier, L., Le Goff, H., Gourcuff, C., Coppola, L., Lavigne, H., Raimbault, P. (2017), A submesoscale coherent vortex in the Ligurian Sea: From dynamical barriers to biological implications, *J. Geophys. Res. Oceans*, 122, 6196–6217, doi:10.1002/2016JC012634.
- Buongiorno Nardelli, B., Guinehut, S., Pascual, A., Drillet, Y., Ruiz, S., & Mulet, S. (2012), Towards high resolution mapping of 3-D mesoscale dynamics from observations. *Ocean Science*, 8(5), 885–901, doi:10.5194/os-8-885-2012.
- Chelton, D. B., P. Gaube, M. G. Schlax, J. A. Early, and R. M. Samelson (2011), The influence of nonlinear mesoscale eddies on near-surface oceanic chlorophyll, *Science*, 334(6054), 328–332, doi:10.1126/science.1208897.

- D'Asaro, E., Lee, C., Rainville, L., Harcourt, R., Thomas, L. (2001), Enhanced turbulence and energy dissipation at ocean fronts, *Science* 322, 318 (2011), doi: 10.1126/science.1201515.
- Fu, L.-L. and R. Ferrari, (2008), Observing Oceanic Submesoscale Processes from Space. *Eos Trans. AGU*, 89(48):488-488.
- Garau, B., S. Ruiz, W. G. Zhang, A. Pascual, E. E. Heslop, J. Kerfoot, and J. Tintoré (2011), Thermal lag correction on Slocum CTD glider data, *J. Atmos. Oceanic Technol.*, 28, 1065–1071.
- Gómez-Navarro, L., Fablet, R., Mason, E., Pascual, A., Mourre, B., Cosme, E., Le Sommer, J. (2018), SWOT Spatial Scales in the Western Mediterranean Sea derived from pseudo-observations and ad hoc filtering. *Remote Sens.*, 10, 599, doi:10.3390/rs10040599.
- Herrmann, M., J. Bouffard, and K. Béranger (2009), Monitoring open-ocean deep convection from space, *Geophys. Res. Lett.*, 36, L03606, doi:10.1029/2008GL036422.
- Hoskins, B. J., Draghici, I. & Davies, H. C. (1978), A new look at the w -equation. *Q. J. Royal Meteorol. Soc.* 104, 31–38, doi:10.1002/qj.49710443903.
- Jaffe, J., Franks, J.S., Roberts, P., Mirza, D., Schurges, C., Kastner, R., Boch, A. (2016), A swarm of autonomous miniature underwater robot drifters for exploring submesoscale ocean dynamics, *Nat. comm.*, 8, 14189, doi:10.1038/ncomms14189.
- Juza, M., B. Mourre, L. Renault, S. Gómara, K. Sebastián, S. Lora, J. P. Beltran, B. Frontera, B. Garau, C. Troupin, M. Torner, E. Heslop, B. Casas, R. Escudier, G. Vizoso, and J. Tintoré (2016), Socib operational ocean forecasting system and multi-platform validation in the western mediterranean sea, *Journal of Operational Oceanography*, 9 (sup1), s155–s166, doi:10.1080/1755876X.2015.1117764.
- Klein, P. & Lapeyre, G (2009), The oceanic vertical pump induced by mesoscale and submesoscale turbulence. *Annu. Rev. Mar. Sci.* 1,351–375, doi:10.1146/annurev.marine.010908.163704.
- Le Traon, P.Y. (2013). From satellite altimetry to Argo and operational oceanography: three revolutions in oceanography. *Ocean Sci.* 9, 901–915, doi:10.5194/os-9-901-2013.
- Lévy, M., P. Klein, and A.-M. Treguier (2001), Impact of sub-mesoscale physics on production and subduction of phytoplankton in an oligotrophic regime., *J. Mar. Res.*, 59,535–565.
- Lumpkin, R., and S. L. Garzoli, (2005), Near-surface circulation in the tropical Atlantic Ocean, In Deep Sea Research Part I: Oceanographic Research Papers, 52, 3, 495-518, doi:10.1016/j.dsr.2004.09.001.
- Mahadevan, A., Olinger, J. & Street, R. A (1996), Nonhydrostatic mesoscale ocean model. Part II: Numerical implementation. *J. Phys. Oceanogr.* 26, 1881–1900.
- Mahadevan, A., A. Tandon, (2006), An analysis of mechanisms for submesoscale vertical motion at ocean fronts. *Ocean Model.* 14, 241.
- Mason, E., A. Pascual, and J.C. McWilliams (2014), A new sea surface height-based code for oceanic mesoscale eddy tracking. *J. Atmos. Oceanic Technol.*, 31, 1181–1188, doi:10.1175/JTECH-D-14-00019.1
- Mason, E., A. Pascual, P. Gaube, S. Ruiz, J. L. Pelegrí, and A. Delepoulle (2017), Subregional characterization of mesoscale eddies across the Brazil-Malvinas Confluence, *J. Geophys. Res. Oceans*, 122, 3329–3357, doi:10.1002/2016JC012611.
- McWilliams, J. C. (2016), Submesoscale currents in the ocean. *Proceedings of the Royal Society of London A: Mathematical, Physical and Engineering Sciences*, 472 (2189), doi:10.1098/rspa.2016.0117.
- Olita, A., Capet, A., Claret, M. et al. *Ocean Dynamics* (2017), Frontal dynamics boost primary production in the summer stratified Mediterranean Sea. *Oce. Dyn.*, 67, 767–782. DOI 10.1007/s10236-017-1058-z.
- Omand, M. M., E. A. D'Asaro, C. M. Lee, M. J. Perry, N. Briggs, I. Cetinic, and A. Mahadevan (2015), Eddy-driven subduction exports particulate organic carbon from the spring bloom, *Science*, doi:10.1126/science.1260062.
- Pascual, A., Faugere, Y., Larnicol, G., and Le Traon, P. Y. (2006), Improved description of the ocean mesoscale variability by combining four satellite altimeters, *Geophys. Res. Lett.*, 33, L02611, doi:10.1029/2005GL024633.
- Pascual, A., Ruiz, S., Martínez-Ledesma, M., Garau, T., Casas, B. Bonet, M., Vidal-Vijande, E., Bouffard, J., Sole, J., Vizoso, G., Orfila, A., Sebastian, K., Buongiorno Nardelli, B., Escudier, R., Schaff, E., Zavala, J., Tintoré, J., (2009), SINOCOP EXPERIMENT: BALEARIC SEA 2009, “A multi-sensor approach”, Technical Report, IMEDEA (CSIC-UIB), 48pp.
- Pascual, A., S. Ruiz, B. Buongiorno Nardelli, S. Guinehut, D. Iudicone, and J. Tintoré (2015), Net primary production in the Gulf Stream sustained by quasi geostrophic vertical exchanges, *Geophys. Res. Lett.*, 42, doi:10.1002/2014GL062569.
- Pascual, A., S. Ruiz, A. Olita, C. Troupin, M. Claret, B. Casas, B. Mourre, P.-M. Poulaïn, A. Tovar-Sánchez, A. Capet, E. Mason, J. T. Allen, A. Mahadevan, and J. Tintoré (2017), A multiplatform experiment to unravel meso- and submesoscale processes in an intense front (AlborEx). *Front. Mar. Sci.* 4, 39, doi:10.3389/fmars.2017.00039.

- Pedder, M. A. (1993), Interpolation and filtering of spatial observations using successive corrections and gaussian filters. *Mon. Weather. Rev.* 121, 2889–2902.
- Pinot, J.-M., Tintoré, J. & Wang, D.-P. (1996), A study of the omega equation for diagnosing vertical motions at ocean fronts. *J. Mar. Res.* 54, 239–259.
- Pollard, R. T., and L. A. Regier (1992), Vorticity and vertical circulation at an ocean front, *J. Phys. Oceanogr.*, 22, 609 –625, doi:10.1175/1520-0485(1992)022<0609:VAVCAA>2.0.CO;2.
- Ramachandran, S., A. Tandon, and A. Mahadevan (2014), Enhancement in vertical fluxes at a front by mesoscale-submesoscale coupling, *Journal of Geophysical Research: Oceans*, 119(12), 8495–8511, doi:10.1002/2014JC010211.
- Rodríguez, J., J. Tintoré, J. Allen, J. Blanco, D. Gomis, A. Reul, J. Ruiz, V. Rodríguez, F. Echevarría, and F. Jiménez-Gómez (2001), Mesoscale vertical motion and the size structure phytoplankton in the ocean. *Nat.* 410, 360–363, doi:10.1029/35066560.
- Rudnick DL (1996) Intensive surveys of the Azores front: 2. Inferring the geostrophic and vertical velocity fields. *J Geophys Res Oceans* 101:16291–16303.
- Ruiz, S., Pascual, A., Garau, B., Pujol, I. & Tintoré, J. (2009a), Vertical motion in the upper ocean from glider and altimetry data. *Geophys. Res. Lett.*, 36., doi:10.1029/2009GL038569. L14607.
- Ruiz S., Pascual A., Garau B., Faugere Y., Alvarez A., Tintoré J. (2009b), Mesoscale dynamics of the Balearic front integrating glider, ship and satellite data. *J. Mar. Syst.* 78: S3-S16.
- Ruiz, S., J. L. Pelegri, M. Emelianov, A. Pascual, and E. Mason (2014), Geostrophic and ageostrophic circulation of a shallow anticyclonic eddy off Cape Bojador, *J. Geophys. Res. Oceans*, 119, 1257–1270, doi:10.1002/2013JC009169.
- Ruiz, S., Pascual A., Casas B., Poulaïn P., Olita A., Troupin C., Torner M., Allen J.T., Tovar-Sánchez A., Mourre B., Massanet A., Palmer M., Margirier F., Balaguer P., Castilla C., Claret M., Mahadevan A., and Tintoré J. (2015), On operation and data analysis from multi-platform synoptic intensive experiment (alborex). *Tech. Rep.* 120pp, doi:10.13140/RG.2.1.3730.4721.
- Ruiz, S., Pascual, A., Mahadevan, A., Claret, M., Olita, A., Troupin, C., Tintoré, J., Poulaïn,, P., Tovar-Sánchez, A., Mourre, B., Capet, A. (2016), Intense ocean frontogenesis inducing submesoscale processes and impacting biochemistry, *Pers. Comm.*, International Liège Colloquium on Submesoscale Processes: Mechanisms, Implications And New Frontiers, 23-27 May 2016, Liège, Belgium.
- Schroeder, K., Gasparini, G. P., Tanghelini, M., and Astraldi, M. (2006), Deep and intermediate water in the western Mediterranean under the influence of the Eastern Mediterranean Transient, *Geophys. Res. Lett.*, 33, L21607, doi:10.1029/2006GL027121.
- Shcherbina, A.Y., M.A. Sundermeyer, E. Kunze, E. D'Asaro, G. Badin, D. Birch, A.E. Brunner-Suzuki, J. Callies, B.T. Kuebel Cervantes, M. Claret, B. Concannon, J. Early, R. Ferrari, L. Goodman, R.R. Harcourt, J.M. Klymak, C.M. Lee, M. Lelong, M.D. Levine, R. Lien, A. Mahadevan, J.C. McWilliams, M.J. Molesmaker, S. Mukherjee, J.D. Nash, T. Özgökmen, S.D. Pierce, S. Ramachandran, R.M. Samelson, T.B. Sanford, R.K. Shearman, E.D. Skillingstad, K.S. Smith, A. Tandon, J.R. Taylor, E.A. Terray, L.N. Thomas, and J.R. Ledwell (2015), The LatMix Summer Campaign: Submesoscale Stirring in the Upper Ocean. *Bull. Amer. Meteor. Soc.*, 96, 1257–1279, doi :10.1175/BAMS-D-14-00015.1.
- Shcherbina, A.Y., E.A. D'Asaro, and S. Nylund (2018), Observing finescale oceanic velocity structure with an autonomous Nortek Acoustic Doppler Current Profiler. *J. Atmos. Oceanic Technol.*, 35, 411–427, doi:10.1175/JTECH-D-17-0108.1.
- Tintoré, J., D. Gomis, S. Alonso, and G. Parrilla (1991), Mesoscale dynamics and vertical motion in the Alboran Sea, *J. Phys. Oceanogr.*, 21, 811–823, doi:10.1175/1520-0485(1991)021<0811:MDAVMI>2.0.CO.

